



## OPEN Nitric oxide donors rescue metabolic and mitochondrial dysfunction in obese Alzheimer's model

Timothy D. Allerton<sup>1</sup>✉, James E. Stampley<sup>2</sup>, Zhen Li<sup>3</sup>, Xiaoman Yu<sup>3</sup>, Heather Quiariate<sup>1,2</sup>, Jake E. Doiron<sup>1</sup>, Ginger White<sup>4</sup>, Zach Wigger<sup>6</sup>, Manas Ranjan Gartia<sup>5</sup>, David J. Lefer<sup>3</sup>, Paul Soto<sup>4</sup> & Brian A. Irving<sup>2</sup>

Reduced nitric oxide (NO) bioavailability is a pathological link between obesity and Alzheimer's disease (AD). Obesity-associated metabolic and mitochondrial bioenergetic dysfunction are key drivers of AD pathology. The hypothalamus is a critical brain region during the development of obesity and dysfunction is an area implicated in the development of AD. NO is an essential mediator of blood flow and mitochondrial bioenergetic function, but the role of NO in obesity-AD is not entirely clear. We investigated diet-induced obesity in female APPswe/PS1dE9 (APP) mouse model of AD, which we treated with two different NO donors (sodium nitrite or L-citrulline). After 26 weeks of a high-fat diet, female APP mice had higher adiposity, insulin resistance, and mitochondrial dysfunction (hypothalamus) than non-transgenic littermate (wild type) controls. Treatment with either sodium nitrite or L-citrulline did not reduce adiposity but improved whole-body energy expenditure, substrate oxidation, and insulin sensitivity. Notably, both NO donors restored hypothalamic mitochondrial respiration in APP mice. Our findings suggest that NO is an essential mediator of whole-body metabolism and hypothalamic mitochondrial function, which are severely impacted by the dual insults of obesity and AD pathology.

Obesity and Alzheimer's disease (AD) are both associated with vascular dysfunction, resulting in reduced peripheral and cerebral blood flow<sup>1–3</sup>. The loss of peripheral nitric oxide (NO) bioavailability corresponds to impaired coronary and cerebrovascular blood flow and microvascular dysfunction that characterizes obesity and AD<sup>4–6</sup>. Notably, the loss of endothelial nitric oxide synthase (eNOS) function promotes amyloid precursor protein accumulation and A $\beta$  plaques in animal models of AD<sup>4</sup>. Furthermore, NO regulates mitochondrial biogenesis and function, serving as a functional mediator of blood flow and metabolism<sup>7</sup>. Mitochondrial dysfunction and reduced NO bioavailability are a shared pathology between obesity and AD that has been hypothesized to play a role in the development of neuropathology and cognitive decline<sup>8</sup>.

Interestingly, obesity in mid-life is considered to be a greater predictor of dementia and AD than late-life obesity<sup>9–11</sup>. Previous reports suggest that brain regions, such as the hypothalamus, that regulate feeding behavior, energy expenditure, and glucose homeostasis, which are intimately associated with the development of obesity, could further exacerbate AD risk<sup>12–14</sup>. Hypothalamic mitochondrial function is critical to maintaining whole-body energy balance and neuronal health<sup>15</sup>. NO is an important signaling molecule in the hypothalamus that preserves mitochondrial bioenergetic and redox balance<sup>16–18</sup>. In animal models of AD, obesity or the partial loss of NO signaling exacerbates neuropathology and cognitive decline<sup>19,20</sup>. In a standard AD mouse model, the APPswe/PS1dE9 (APP) mouse, demonstrates significant alternations in plasma L-arginine (NO substrate) and hippocampus and prefrontal cortex at mid-life<sup>21</sup>. However, no data demonstrates if obesity exacerbates mitochondrial dysfunction in the hypothalamus of AD patients or animal models. A greater understanding of hypothalamic mitochondrial function and the role of nitric oxide in AD is critically important given the strong association between obesity and AD.

<sup>1</sup>Vascular Metabolism Laboratory, Pennington Biomedical Research Center, Baton Rouge, LA 70808, USA.

<sup>2</sup>Department of Kinesiology, Louisiana State University, Baton Rouge, LA, USA. <sup>3</sup>Department of Cardiac Surgery, Smidt Heart Institute, Cedars-Sinai Medical Center, Los Angeles, CA, USA. <sup>4</sup>Department of Psychology, Louisiana State University, Baton Rouge, LA, USA. <sup>5</sup>Department of Mechanical and Industrial Engineering, Louisiana State University, Baton Rouge, LA, USA. <sup>6</sup>Adipocyte Biology Laboratory, Pennington Biomedical Research Center, Baton Rouge, LA, USA. ✉email: timothy.allerton@pbrc.edu

Mitochondrial dysfunction and reduced NO bioavailability are potential forerunners for the development of A $\beta$  plaque formation<sup>8,22</sup>. These studies demonstrate an essential shared metabolic underpinning between obesity and AD. Obesity in mid-life, before overt plaque formation, tau accumulation, and cognitive decline represents a critical time point that sets the stage for late-life AD development. Therefore, we focused our investigation on the metabolic aspects of obesity and mitochondrial function prior to late-life AD. We hypothesized that NO donors, aimed at restoring global NO bioavailability, therapy would attenuate metabolic dysfunction in female APP mice with diet-induced obesity.

## Results

### Body composition and biomarkers of metabolic health in APP mice

Figure 1 illustrates the experimental design. Female APP mice and wild-type (WT) littermate controls (10 weeks of age) were fed a standard chow diet or 45% HFD for 26 weeks. A group of APP HFD mice were randomized to groups with standard drinking water, sodium nitrite (100 mg/L) drinking water, or L-citrulline (440 mg/L). Body mass (Fig. 2A) and body fat (Fig. 2B) were significantly greater in APP HFD mice when compared to WT HFD mice. A significant reduction was detected in the percentage of lean body mass (Fig. 2C) in HFD groups but with no difference between WT and APP mice. APP mice were more glucose intolerant compared to control animals (Fig. 2D, E) but did not improve with sodium nitrite or L-citrulline treatment. Insulin tolerance (AUC) was also reduced in APP HFD mice compared to the control group but increased with sodium nitrite and L-citrulline treatment (Fig. 2F, G). Plasma insulin (Fig. 2H), was increased between APP chow and APP HFD, but not between WT chow and WT HFD mice ( $p=0.30$ ). Plasma leptin (Fig. 2I) was increased in HFD groups for WT and APP, but with no effect of sodium nitrite or L-citrulline. Plasma nitrite was measured to determine global nitric oxide bioavailability. Only APP HFD mice treated with L-citrulline (Fig. 2J) demonstrated statistical increases in plasma nitrite. While sodium nitrite treatment numerically increased plasma nitrite there was no statistical difference ( $p=0.67$ ).

### Whole-body energy expenditure and substrate oxidation

Using ANCOVA, we detected a significant increase in total energy expenditure (TEE) in APP HFD mice when compared to WT HFD. Both sodium nitrite and L-citrulline treatments also significantly increase TEE (Fig. 3A, B). The respiratory exchange ratio (RER) was lower in sodium nitrite and L-citrulline-treated APP mice (Fig. 3C, D). Fat oxidation (Fig. 3E) increased, in L-citrulline versus untreated APP HFD mice. Total physical activity in the cage only differed between WT chow versus HFD mice (Fig. 4D-F). No differences were detected for any whole-body metabolic parameters when comparing APP mice versus control mice fed a chow diet. The behavioral analysis collected during the metabolic cage experiment indicates APP HFD mice did not have any significant differences in activities related to eating or drinking but did spend a great percentage of time in long lounging (LLnge) compared to WT HFD mice. When compared directly APP HFD mice average greater amounts of movement in the cage (WT HFD  $235 \pm 48$  vs. APP HFD  $296 \pm 54$ ,  $p=0.04$ ) There was no significant difference in total food or water intake (Supplemental Fig. 1).

### Nitric oxide donors rescue hypothalamic mitochondrial dysfunction in obese APP mice

Respiration of hypothalamus homogenates for  $N_L$  (NADH-linked LEAK) did not differ between groups (Fig. 4A).  $N_p$  (NADH-linked OXPHOS) was reduced in APP HFD versus WT HFD mice but was restored with sodium nitrite treatment (Fig. 4B). Sodium nitrite and L-citrulline treatment restored respiration in APP

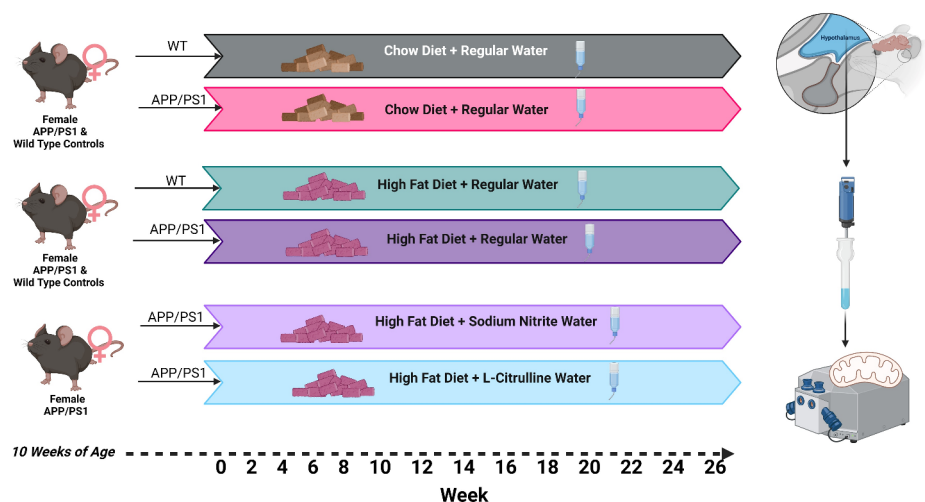


**Fig. 1.** Experimental Design.

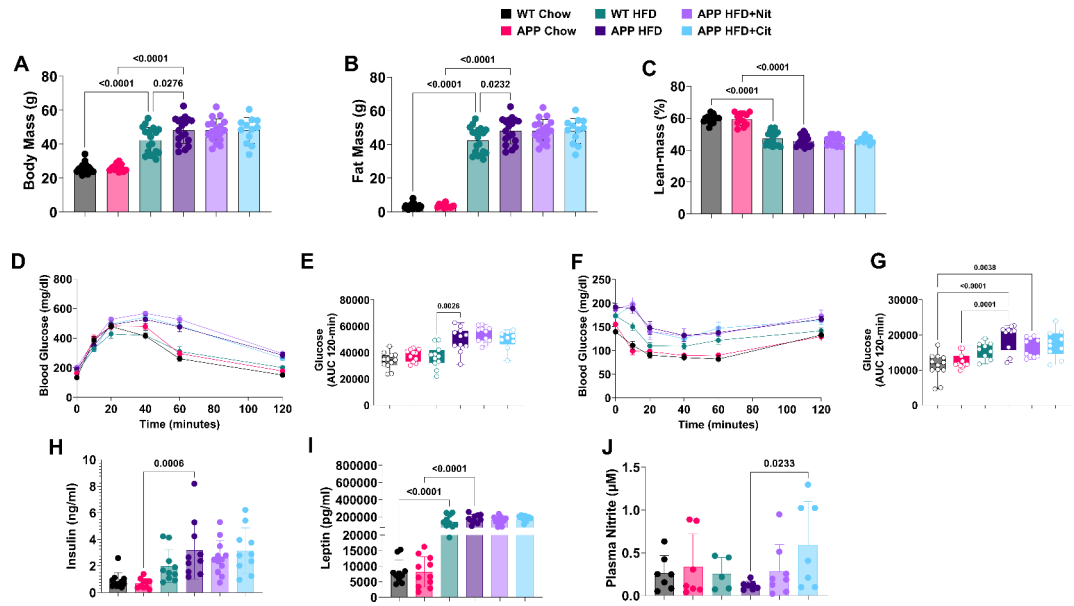


**Fig. 2.** APP mice have exacerbated obesity and metabolic dysfunction on a HFD. (A) Final body weight, (B) body fat, and (C) percent lean mass. (E) Glucose curves and (F) area under the curve for glucose tolerance test. (G) Glucose curve and (H) area under the curve for insulin tolerance test. Fasting plasma (I) insulin, (J) leptin, and (K) nitrite. One-way ANOVA was used to determine group effects with Tukey’s test for multiple comparisons. WT Chow ( $n=13-20$ ), APP Chow ( $n=12$ ), WT HFD ( $n=9-19$ ), APP HFD ( $n=7-18$ ), APP + Nit ( $n=10-18$ ), APP + Cit ( $n=9-12$ ). Data are reported as mean  $\pm$  SD.

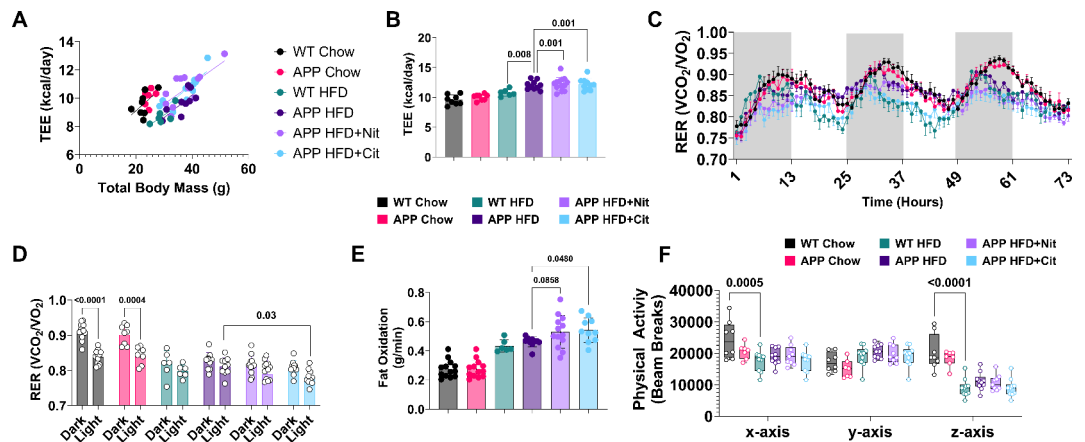


**Fig. 3.** Nitric oxide donors increase metabolic rate and shift substrate utilization towards fat oxidation. (A, B) Total body energy expenditure (TEE) for all groups. (C) Three-day representation of the respiratory exchange ratio (RER) and (D) RER average separated by dark and light cycle. (E) Absolute average fat oxidation. (F) Physical activity beam breaks. ANOVA with total body mass covariate was used to determine the difference in total energy expenditure. One-way ANOVA was used to determine group effects with Tukey’s test for multiple comparisons. WT Chow ( $n=13$ ), APP Chow ( $n=8$ ), WT HFD ( $n=6$ ), APP HFD ( $n=11$ ), APP HFD + Nit ( $n=10$ ), APP HFD + Cit ( $n=10$ ). Data are reported as mean  $\pm$  SD. #, indicate significant group effects according to ANCOVA.

HFD mice from NSp (NADH & Succinate-linked OXPHOS) (Fig. 4C), NS<sub>E</sub> (NADH&Succinate-linked ET capacity) (Fig. 4D) S<sub>E</sub> (Succinate-linked ET capacity) (Fig. 4E), and SG<sub>E</sub> (Succinate & Glycerol Phosphate-linked ET capacity) (Fig. 4F). RCR (OXPHOS/LEAK) for NADH-linked respiration (Fig. 4G) was also reduced in APP HFD mice but was attenuated with sodium nitrite treatment. When compared directly, APP mice a chow diet, showed a reduction in OXPHOS (NS<sub>p</sub>) and ET capacity (NS<sub>E</sub>) when compared to WT chow-fed mice (Supplemental Fig. 2).

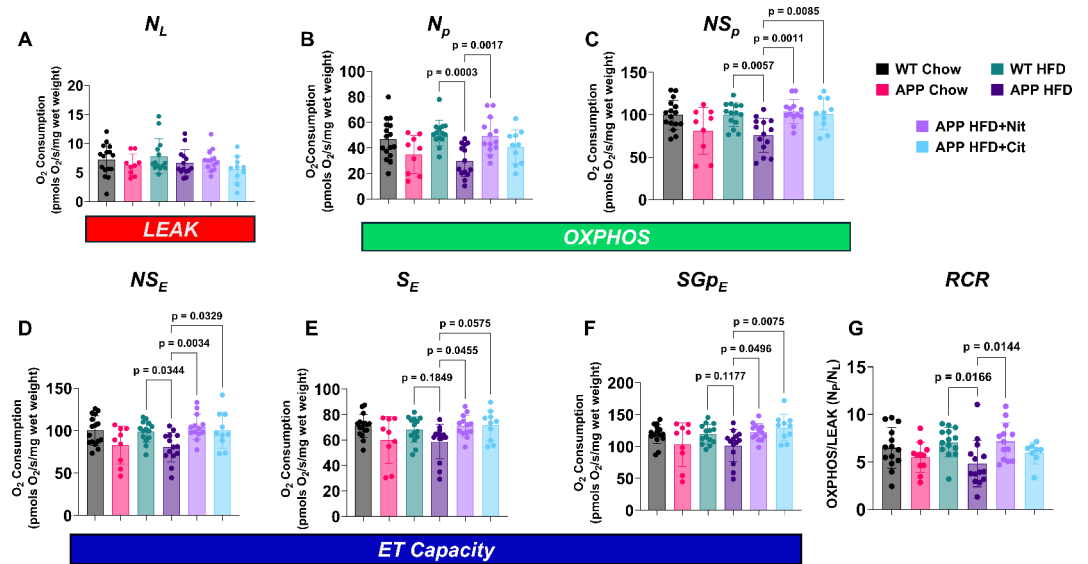


**Fig. 4.** Nitric oxide donor reverses mitochondrial dysfunction in obese APP mice. (A)  $N_L$  (NADH-linked LEAK), (B)  $N_p$  (NADH-linked OXPHOS capacity), (C)  $NS_p$  (NADH&Succinate-linked OXPHOS capacity), (D)  $NS_E$  (NADH&Succinate-linked ET capacity), (E)  $S_E$  (Succinate-linked ET capacity), (F)  $SGp_E$  (Succinate-&Glycerol Phosphate-linked ET capacity), and the (G) respiratory control ratio (RCR, OXPHOS/LEAK for NADH-linked respiration). Measurements were made using high-resolution respirometry at 37 °C with  $O_2$  concentrations between ~450  $\mu M$  and ~150  $\mu M$ , see methods for more details on the overall titration protocol. One-way ANOVA was used to determine group effects with Tukey's test for multiple comparisons. WT HFD ( $n = 14$ ), APP HFD ( $n = 14$ ), APP HFD + Nit ( $n = 11$ ), APP HFD + Cit ( $n = 10$ ). Data are reported as mean  $\pm$  SD.

## Discussion

In this proof-of-concept study, we investigated the capacity of NO donors to restore metabolic function in an obese transgenic mouse model of AD. Obesity, particularly in mid-life, is a major risk factor for developing future AD<sup>2,11,23</sup>. We focused our investigation on obese female APP mice before the accumulation of A $\beta$  plaques (9–12 months) as this timeframe appears to set the stage for late-life AD-related defects. Reduced NO bioavailability from obesity potentially increases the risk of developing AD<sup>24</sup>. Our results confirm previous observations that APP mice have exacerbated obesity (Fig. 2A, B) when fed a HFD<sup>25–28</sup>. While we did not observe any beneficial effects of NO donor therapies on body composition or glucose tolerance, insulin sensitivity was improved with both NO donors (Fig. 2G–H). This is not surprising given data regarding the impact of NO therapies have conflicting results on metabolic outcomes<sup>29</sup>. Compared to male mice, female mice are generally protected from obesity-related metabolic dysfunction. In our study, female APP mice demonstrate exacerbated insulin resistance on a HFD suggesting that mutations in amyloid precursor protein and presenilin-1 exacerbate metabolic dysfunction in mid-life. Our data also demonstrate some beneficial effects of NO donor therapy on metabolic outcomes in APP HFD mice.

Some studies have demonstrated that patients with AD have altered energy expenditure when compared to health age-matched controls<sup>30–32</sup>. In our investigation, TEE was not different between chow-fed WT and APP mice but was increased in APP mice on a HFD. NO donor therapy further increased TEE when compared to untreated APP mice (Fig. 3A–F). Additionally, L-citrulline reduced RER suggesting a shift a more prominent shift towards fat oxidation. Despite the increase in TEE and fat oxidation (Fig. 3D), these NO donors (sodium nitrite & L-citrulline) did not alter body composition. This is likely due to the small increase in food intake measured throughout the experiment and during the metabolic cage study. NO has been shown to promote food intake in some animal models and may potentially counteract the gain in energy expenditure by increasing energy intake<sup>17</sup>. One feature of APP mice reporter in late life is increased anxiety-like behavior. While the age of our mice and our analytical approach did not allow us to evaluate this aspect we did detect an increase in total amulation in the metabolic cage experiment in APP HFD mice. The increase in movement could potentially explain the increase in TEE in the APP HFD mice.

Mitochondrial dysfunction is one emerging hypothesis to explain the development of AD pathology<sup>33</sup>. Mitochondrial dysfunction is prominently featured in the underlying pathophysiology of obesity and insulin resistance. However, how mitochondrial dysfunction impacts the relationship between obesity and AD development is poorly understood. Signatures of mitochondrial damage, gene regulation, and oxidative stress are associated with AD in at-risk populations<sup>34,35</sup>. Mitochondrial function of the hypothalamus was our primary outcome of interest. The hippocampus is crucial for the development of cognitive aspects of AD, but how it mediates the burden of obesity and associated risk factors is unclear. Obesity does not appear to uniformly and negatively affect hippocampal function and inflammation<sup>36–38</sup>. Whereas, the hypothalamus is the brain region responsible for energy balance and is implicated in AD development<sup>39,40</sup>. Work in animal models has

revealed that loss of eNOS/NO function is an early defect that precedes neurodegeneration and behavioral dysfunction in AD<sup>4,6,24</sup>. Obesity is associated with hypertension and metabolic dysfunction that are strongly dependent on eNOS/NO function. Ours is the first study to report reduced respiration from the hypothalamus in obese APP mice. While there was some diminution of mitochondrial function in chow-fed APP mice this effect was exacerbated on a high-fat diet when compared to WT HFD mice.  $N_p$ ,  $NS_p$ ,  $NS_E$ , and RCR were reduced in APP HFD mice relative to WT HFD mice. Treatment with sodium nitrite restored all respiratory states, including RCR, to control levels. In addition, sodium nitrite also increased  $S_E$  and  $SGp_E$  in the APP HFD mice despite no significant reduction when compared to WT HFD mice. Whereas L-citrulline also broadly increased mitochondrial respiration, but with a non-significant impact on  $N_p$  respiration and RCR. We demonstrate restoring NO bioavailability is critical to reverse this metabolic defect in the hypothalamus. We demonstrate the clear and robust ability of two different NO donors to rescue hypothalamic mitochondrial function, which is a key factor in the development of obesity and metabolic disease<sup>40</sup>. A recent report suggests that APP/PS1 mice with a partial knockout of eNOS<sup>+/-</sup> developed a more severe AD phenotype than eNOS intact APP/PS1 mice<sup>20</sup>. Another study also demonstrated that the pharmacological inactivation of eNOS using L-NAME in APP/PS1 mice also resulted in greater amyloid burden and cognitive impairment, further supporting the importance of NO bioavailability in the development of the AD phenotype within the APP/PS1 model<sup>20,41</sup>. Although these two studies did not measure changes in mitochondrial content or function, their results highlight the potential role of NO bioavailability as a mediator of AD vascular and perhaps mitochondrial dysfunction.

Obesity in mid-life, but not late life, increases the risk of developing future AD<sup>3,10,11,42</sup>. A strength of our study is we investigated adult, but not elderly, mice at a period considered critical for the exacerbating effects of obesity on AD development. The substantial and broad hypothalamic mitochondrial dysfunction we detected during obesity and mid-life is a novel finding. Additionally, we utilized female mice in this study. Approximately two-thirds of AD patients are women<sup>43</sup>. This could potentially be attributed to the greater longevity of women and the impact of aging on AD<sup>44</sup>. However, the dual insults of obesity and menopause reduce NO bioavailability independent of one another. The significant loss of NO function is a plausible precursor to peripheral and metabolic dysfunction. Last, the use of two different NO donors strengthens our findings. Sodium nitrite and L-citrulline work via non-enzymatic and enzymatic routes, respectively, to produce NO. Both NO donors have been shown to increase NO bioavailability significantly<sup>45–48</sup>. In our study, only L-citrulline demonstrated a statistical increase in plasma nitrite. However, sodium nitrite is a powerful NO donor and the lack of increase from this therapy may indicate greater nitrite reduction to free NO. Our findings demonstrate that targeting NO bioavailability via the enzymatic (L-citrulline) and non-enzymatic (sodium nitrite) routes effectively restored mitochondrial function.

Despite the strengths of our study, it is not without limitations. Our primary focus was to investigate the metabolic aspects of AD. Therefore, we do not have information regarding brain pathology. We did not investigate mitochondrial function in brain regions such as the hippocampus or the cortex which are more commonly implicated in neurodegeneration during AD. Additionally, we only investigated younger mice (10 weeks of age) fed a HFD for 26 weeks. APP mice acquire AD-related behavioral dysfunction much later in life (12–17 months of age). Therefore, the durability of NO donor therapy to rescue metabolic dysfunction in a mouse model of AD will require more extended treatment periods. The APP mouse itself is also a potential limiting factor in that it only represents one aspect of the AD pathology (i.e., A $\beta$  accumulation). Whether our treatment would extend benefit to other mouse models of AD that encompass more aspects of AD pathology remains to be answered. Finally, we only studied female mice; while this is also a major strength due to the prevalence of AD in women and the paucity of data in female AD models, we are unable to determine the impact of sex on our outcomes directly.

In summary, we have provided novel evidence of obesity-induced mitochondrial dysfunction in young female APP mice. We demonstrate that increased NO bioavailability via two different pathways rescues metabolic and mitochondrial dysfunction. These findings highlight the importance of NO supplementation and strategies, such as healthy diet and exercise, to preserve NO bioavailability during mid-life when obesity has its greatest impact on AD progression.

## Methods

### Animal model and experimental design

Female transgenic APP<sup>swe</sup>/PS1<sup>dE9</sup> (APP) ( $n=60$ ) and non-transgenic littermate controls (Control,  $n=20$ ) were purchased from Jackson Laboratory (Bar Harbor, ME) at 8 weeks of age. Mice were acclimated for two weeks and were then placed on a high-fat diet (45% HFD, Research Diets 12451, New Brunswick, NJ) or a standard chow diet (Purina 5001). High-fat diet-fed APP mice were randomized to either standard water, sodium nitrite (100 mg/L) water, or L-citrulline (400 mg/L) drinking water with *ad libitum* access. Littermate control was provided with standard drinking water in addition to the HFD. Food intake and body mass were measured weekly. Body composition was acquired by NMR every two weeks. Metabolic cages experiments were conducted between weeks 23–24. Glucose and insulin tolerance testing was performed between weeks 24–25 and 25–26, respectively. Some mice were removed from the protocol due to sudden death, which is common in this strain, or skin lesions that required treatment and removal from the protocol. Mice were euthanized by isoflurane administration with cardiac puncture. The Pennington Biomedical Research Center Institution Animal Care and Use Committee approved all experiments. All methods were performed in accordance with the relevant guidelines and regulations. The study is reported in accordance with ARRIVE guidelines.

## Metabolic cages

One week before metabolic cage experiments, mice were acclimated to single-housed training cages. Mice were placed in metabolic cages (Sable Systems, Promethion, Las Vegas, NV) for seven days. Oxygen consumption ( $\text{VO}_2$ ) and carbon dioxide production ( $\text{VCO}_2$ ) were monitored constantly. Standard equations were used to calculate fat oxidation<sup>49</sup>. Physical activity, food, and water uptake behaviors were monitored and recorded in 5-minute intervals. Physical and behavioral activity (eating, drinking, resting) were continuously monitored by beam breaks (x, y, and z-axes). Behavioral analysis was performed using Sables Systems Ethoscan.

## Metabolic tolerance tests and cardiometabolic biomarkers

Glucose tolerance testing was conducted after a 4-hour fast, during which baseline blood was collected by tail vein nick and measured with a handheld glucometer (Breeze2 glucometer, Leverkusen, Germany). Interperitoneal injection of glucose (3.5 g/kg lean body mass) was performed, and blood was collected (tail vein) 15, 30, 60, 45, 90, and 120 min thereafter. On a separate week, mice were fasted for 2 h, and baseline blood was measured. Interperitoneal injection of insulin (1.5 units/kg, Humulin; Eli Lilly, Indianapolis, IN) was injected, and blood was collected 10, 20, 40, 60, and 120 min thereafter. The area of the curve was calculated using the trapezoidal method. Fasting insulin (Crystal Chem, 90080) and leptin were analyzed by ELISA (Invitrogen, 900-K76K) according to the manufacturer's instructions. Circulating nitrite concentrations were determined as previously described<sup>50</sup>. Briefly, plasma samples were incubated with an equal volume of methanol for 2 min and then centrifuged at 21,000 g for 15 min. The supernatant then was analyzed with a specialized HPLC-based NOx analyzer (ENO-30, Amuza Inc., San Diego, US) using Griess Reaction as the principle.

### High-Resolution Respirometry.

Following euthanasia, the hypothalami were carefully dissected and placed in an ice-cold biopsy preservation buffer (BIOPS, 10 mM Ca-EGTA buffer, 0.1  $\mu\text{M}$  free calcium, 20 mM imidazole, 20 mM taurine, 50 mM K-MES, 0.5 mM DTT, 6.56 mM  $\text{MgCl}_2$ , 5.77 mM ATP, 15 mM phosphocreatine, pH 7.1). Subsequently, the hypothalami were homogenized in an ice-cold mitochondrial respiration buffer (MiR05 kit, Oroboros, Austria, 0.5 mM EGTA, 3 mM  $\text{MgCl}_2$ , 60 mM Lactobionic Acid, 20 mM Taurine, 10 mM  $\text{KH}_2\text{PO}_4$ , 20 mM HEPES, 110 mM Sucrose, 1 g/L Fatty Acid-Free bovine serum albumin, pH 7.1) at 150 revolutions per minute for 60 s in plastic-coated glass tubes on ice using glass pestles with a clearance of 0.10–0.15 mm. After homogenization, the hypothalamic homogenates were transferred to two 2 mL high-resolution respirometry chambers (HRR, Oroboros O2k, Austria) with MiR05 for duplicate measurements (~0.5–1.5 mg per chamber). HRR coupled with a standardized substrate-uncoupler-inhibitor-titration (SUIT) protocol was used to measure respiration rates in the following coupling control states (State 4), OXPHOS capacity ( $\geq$  State 3), and electron transfer (ET) capacity. All measurements were made at 37 °C and  $\text{O}_2$  concentrations between ~450  $\mu\text{M}$  and ~150  $\mu\text{M}$  in MiR05 supplemented with  $\alpha$ -chaconine (40  $\mu\text{M}$ ) to chemically permeabilize the plasma membranes and synaptosomes<sup>51</sup>. NADH-linked LEAK respiration ( $N_L$ ) was measured in the presence of 5 mM pyruvate, 2 mM malate, and 10 mM glutamate without ADP. NADH-Linked OXPHOS ( $N_p$ ) was measured after adding 5 mM ADP-Mg<sup>++</sup>. Mitochondrial membrane integrity was assessed after adding 10  $\mu\text{M}$  cytochrome c. NADH&Succinate-linked OXPHOS ( $NS_p$ ) respiration was measured after adding 10 mM succinate. Next, carbonyl cyanide m-chlorophenyl hydrazine (CCCP) was titrated using 0.5  $\mu\text{M}$ /step to measure NADH&Succinate-linked ET capacity ( $NS_E$ ) respiration. Next, 0.5  $\mu\text{M}$  rotenone was added to measure Succinate-linked ET capacity ( $S_E$ ) respiration, followed by the titration of 15 mM glycerol-3-phosphate (Gp) to measure Succinate&Gp-linked ET capacity ( $SG_{pE}$ ) respiration. Finally, 2.5  $\mu\text{M}$  antimycin A was added to measure residual oxygen consumption (Rox). The respiration rates were normalized per mg mass [ $\text{pmol}\cdot\text{s}^{-1}\cdot\text{mg}^{-1}$ ] after correcting for Rox, referred to as oxygen flux ( $J_{\text{O}_2}$ ). HRR measurements were corrected for daily room air calibration, routine background, and zero calibrations. All HRR measurements and analyses were made in a blinded fashion.

## Statistical analysis

The normality of data were assessed by the D'Agostino and Pearson test. One-way ANOVA was used to determine group differences with Tukey's tests for multiple comparisons. ANCOVA was performed to determine differences in energy expenditure with total body factored as a co-variate. Simple linear regression was used to determine correlations. Statistical analysis was performed with GraphPad (Prism version 10.2.0, GraphPad Software, Boston, Massachusetts, USA) and JMP<sup>®</sup> PRO software (Version 16, Cary, NC). All values are reported as mean  $\pm$  standard deviation (SD). Significance was determined a  $P < 0.05$ .

## Data availability

Data will be available upon a reasonable request to Dr. Timothy Allerton (timothy.allerton@pbrc.edu).

Received: 12 March 2024; Accepted: 8 October 2024

Published online: 30 October 2024

## References

- Scheffer, S., Hermkens, D. M. A., Van Der Weerd, L., De Vries, H. E. & Daemen, M. J. A. P. Vascular hypothesis of Alzheimer Disease: Topical review of mouse models. *Arterioscler. Thromb. Vasc Biol.* 1265–1283. <https://doi.org/10.1161/ATVBAHA.120.311911> (2021).
- Kivipelto, M. et al. Obesity and vascular risk factors at midlife and the risk of dementia and Alzheimer disease. *Arch. Neurol.* **62**, 1556–1560 (2005).
- Dove, A. et al. Cardiometabolic multimorbidity accelerates cognitive decline and dementia progression. *Alzheimer's Dement.* <https://doi.org/10.1002/ALZ.12708> (2022).

4. Austin, S. A., Santhanam, A. V., Hinton, D. J., Choi, D. S. & Katusic, Z. S. Endothelial nitric oxide deficiency promotes Alzheimer's disease pathology. *J. Neurochem.* **127**, 691–700 (2013).
5. De La Torre, J. C. & Stefano, G. B. Evidence that Alzheimer's disease is a microvascular disorder: The role of constitutive nitric oxide. *Brain Res. Rev.* **34**, 119–136 (2000).
6. De La Monte, S. M., Sohn, Y. K., Etienne, D., Kraft, J. & Wands, J. R. Role of aberrant nitric oxide synthase-3 expression in cerebrovascular degeneration and vascular-mediated injury in Alzheimer's disease. *Ann. N Y Acad. Sci.* **903**, 61–71 (2000).
7. Nisoli, E. et al. Mitochondrial biogenesis in mammals: The role of endogenous nitric oxide. *Sci. (80-)*. **299**, 896–899 (2003).
8. Cenini, G. & Voos, W. Mitochondria as potential targets in Alzheimer disease therapy: An update. *Front. Pharmacol.* **10**, 1–20 (2019).
9. Toda, N. & Okamura, K. A. Obesity-Induced Cerebral Hypoperfusion derived from endothelial dysfunction: One of the risk factors for Alzheimer's Disease. *Curr. Alzheimer Res.* **11**, 733–744 (2014).
10. Anstey, K. J., Cherbuin, N., Budge, M. & Young, J. Body mass index in midlife and late-life as a risk factor for dementia: A meta-analysis of prospective studies. *Obes. Rev.* **12**, 426–437 (2011).
11. Nepal, B., Brown, L. J. & Anstey, K. J. Rising midlife obesity will worsen future prevalence of dementia. *PLoS One* **9**, (2014).
12. McDuff, T. & Sumi, S. M. Subcortical degeneration in Alzheimer's disease. *Neurology.* **35**, 123–126 (1985).
13. Saper, C. B. & German, D. C. Hypothalamic pathology in Alzheimer's disease. *Neurosci. Lett.* **74**, 364–370 (1987).
14. Schultz, C., Ghebremedhin, E., Braak, H. & Braak, E. Neurofibrillary pathology in the human paraventricular and supraoptic nuclei. *Acta Neuropathol.* **94**, 99–102 (1997).
15. Jin, S. & Diano, S. Mitochondrial dynamics and hypothalamic regulation of metabolism. *Endocrinology.* **159**, 3596–3604 (2018).
16. Sakamuri, S. S. V. P. et al. Nitric oxide synthase inhibitors negatively regulate respiration in isolated rodent cardiac and brain mitochondria. *Am. J. Physiol. Heart Circ. Physiol.* **318**, H295–H300 (2020).
17. Han, C., Zhao, Q. & Lu, B. The role of nitric oxide signaling in food intake; insights from the inner mitochondrial membrane peptidase 2 mutant mice. *Redox Biol.* **1**, 498–507 (2013).
18. Gyengesi, E., Paxinos, G. & Andrews, Z. B. Oxidative stress in the Hypothalamus: The importance of Calcium Signaling and mitochondrial ROS in Body Weight Regulation. *Curr. Neuropharmacol.* **10**, 344–353 (2012).
19. Hamilton, A. & Holscher, C. The effect of ageing on neurogenesis and oxidative stress in the APP swe/PS1 deltaE9 mouse model of Alzheimer's disease. *Brain Res.* **1449**, 83–93 (2012).
20. Ahmed, S. et al. Partial endothelial nitric oxide synthase deficiency exacerbates cognitive deficit and amyloid pathology in the APPswe/PS1ΔE9 mouse model of Alzheimer's Disease. *Int. J. Mol. Sci.* **23**, (2022).
21. Bergin, D. et al. Altered plasma arginine metabolome precedes behavioural and brain arginine metabolomic profile changes in the APPswe/PS1ΔE9 mouse model of Alzheimer's disease. *Transl Psychiatry* **8**, (2018).
22. Leuner, K., Müller, W. E. & Reichert, A. S. From mitochondrial dysfunction to amyloid beta formation: Novel insights into the pathogenesis of Alzheimer's disease. *Mol. Neurobiol.* **46**, 186–193 (2012).
23. Walker, J. M. & Harrison, F. E. Shared neuropathological characteristics of obesity, type 2 diabetes and Alzheimer's disease: Impacts on cognitive decline. *Nutrients.* **7**, 7332–7357 (2015).
24. Asimwe, N., Yeo, S. G., Kim, M. S., Jung, J. & Jeong, N. Y. Nitric oxide: Exploring the contextual link with Alzheimer's disease. *Oxid. Med. Cell. Longev.* (2016). (2016).
25. Thériault, P., ElAli, A. & Rivest, S. High fat diet exacerbates Alzheimer's disease-related pathology in APPswe/PS1 mice. *Oncotarget.* **7**, 67808–67827 (2016).
26. Bracko, O. et al. High fat diet worsens Alzheimer's disease-related behavioral abnormalities and neuropathology in APP/PS1 mice, but not by synergistically decreasing cerebral blood flow. *Sci. Rep.* **10**, 1–16 (2020).
27. Ettcheto, M. et al. Evaluation of neuropathological effects of a high-fat diet in a presymptomatic alzheimer's disease stage in APP/PS1 mice. *J. Alzheimers Dis.* **54**, 233–251 (2016).
28. Lee, Y. H. et al. Augmented insulin and leptin resistance of high fat diet-fed APPswe/PS1ΔE9 transgenic mice exacerbate obesity and glycemic dysregulation. *Int. J. Mol. Sci.* **19**, (2018).
29. Cau, S. B. A., Carneiro, F. S. & Tostes, R. C. Differential modulation of nitric oxide synthases in aging: Therapeutic opportunities. *Front. Physiol.* **3 JUN**, (2012).
30. Zou, Y., Wang, Q. & Cheng, X. Causal relationship between basal metabolic rate and Alzheimer's Disease: Abidirectional two-sample mendelian randomization study. *Neurol. Ther.* **12**, 763–776 (2023).
31. Doorduyn, A. S. et al. Energy intake and expenditure in patients with Alzheimer's disease and mild cognitive impairment: The NUDAD project. *Alzheimer's Res. Ther.* **12**, 1–8 (2020).
32. Poehlman, E. T. & Dvorak, R. V. Energy expenditure, energy intake, and weight loss in Alzheimer disease. *Am. J. Clin. Nutr.* **71**, 650S–655S (2000).
33. Zou, D. et al. Single-cell and spatial transcriptomics reveals that PTPRG activates the m6A methyltransferase VIRMA to block mitophagy-mediated neuronal death in Alzheimer's disease. *Pharmacol. Res.* **201**, 107098 (2024).
34. Reid, D. M. et al. Integrative blood-based characterization of oxidative mitochondrial DNA damage variants implicates Mexican American's metabolic risk for developing Alzheimer's disease. *Sci. Rep.* **13**, 1–15 (2023).
35. Giannos, P., Prokopidis, K., Raleigh, S. M., Kelaiditi, E. & Hill, M. Altered mitochondrial microenvironment at the spotlight of musculoskeletal aging and Alzheimer's disease. *Sci. Rep.* **12**, 1–8 (2022).
36. Leyh, J. et al. Long-term diet-induced obesity does not lead to learning and memory impairment in adult mice. *PLoS ONE* **16**, (2021).
37. Osiecka, Z. et al. Obesity reduces hippocampal structure and function in older African americans with the APOE-ε4 Alzheimer's disease risk allele. *Front. Aging Neurosci.* **15**, (2023).
38. Letra, L., Santana, I. & Seica, R. Obesity as a risk factor for Alzheimer's disease: The role of adipocytokines. *Metab. Brain Dis.* **29**, 563–568 (2014).
39. Zheng, H. et al. The hypothalamus as the primary brain region of metabolic abnormalities in APP/PS1 transgenic mouse model of Alzheimer's disease. *Biochim. Biophys. Acta - Mol. Basis Dis.* **1864**, 263–273 (2018).
40. Cunarro, J., Casado, S., Lugalde, J. & Tovar, S. Hypothalamic mitochondrial dysfunction as a target in obesity and metabolic disease. *Front. Endocrinol. (Lausanne)*. **9**, 1–10 (2018).
41. Cifuentes, D. et al. Inactivation of nitric oxide synthesis exacerbates the development of Alzheimer Disease Pathology in APPPS1 mice (amyloid precursor Protein/Presenilin-1). *Hypertens. (Dallas Tex. 1979)*. **70**, 613–623 (2017).
42. Anjum, I., Fayyaz, M., Wajid, A., Sohail, W. & Ali, A. Does obesity increase the risk of dementia: A literature review. *Cureus* **10**, (2018).
43. Scheyer, O. et al. Female sex and Alzheimer's risk: The menopause connection. *J. Prev. Alzheimer's Dis.* **5**, 225–230 (2018).
44. Castro-Aldrete, L. et al. Sex and gender considerations in Alzheimer's disease: The women's Brain Project contribution. *Front. Aging Neurosci.* **15**, 1–12 (2023).
45. Powers, R. et al. L-Citrulline administration increases the arginine/ADMA ratio, decreases blood pressure and improves vascular function in obese pregnant women. *Pregnancy Hypertens.* <https://doi.org/10.1016/j.preghy.2014.10.011> (2015).
46. Schwedhelm, E. et al. Pharmacokinetic and pharmacodynamic properties of oral L-citrulline and L-arginine: Impact on nitric oxide metabolism. *Br. J. Clin. Pharmacol.* **65**, 51–59 (2008).
47. Bryan, N. S. Nitrite in nitric oxide biology: Cause or consequence? A systems-based review. *Free Radic. Biol. Med.* <https://doi.org/10.1016/j.freeradbiomed.2006.05.019> (2006).

48. Bryan, N. S. et al. Nitrite is a signaling molecule and regulator of gene expression in mammalian tissues. *Nat. Chem. Biol.* <https://doi.org/10.1038/nchembio734> (2005).
49. Jéquier, E., Acheson, K. & Schutz, Y. Assessment of energy expenditure and fuel utilization in man. *Annu. Rev. Nutr.* <https://doi.org/10.1146/annurev.nu.07.070187.001155> (1987).
50. King, A. L. et al. Hydrogen sulfide cytoprotective signaling is endothelial nitric oxide synthase-nitric oxide dependent. *Proc. Natl. Acad. Sci. U S A.* <https://doi.org/10.1073/pnas.1321871111> (2014).
51. Dawid, C. et al. Comparative assessment of purified saponins as permeabilization agents during respirometry. *Biochim. Biophys. Acta Bioenerg.* **1861**, 148251 (2020).

## Acknowledgements

The authors thank Tamra Mendoza for her assistance with animal care. The authors thank the Pennington Animal Metabolism and Behavioral Core supported by NIH P20 GM135002, P20 GM103528, and P30 DK072476 for assistance with metabolic cage experiments.

## Author contributions

Data collection (T.D.A, H.Q., J.E.S., M.G., B.A.I., P.S., Z.W., Z.L., X.Y, J.E.D., G.W.), Data analysis (T.D.A, M.G., D.J.L. & B.A.I), initial draft (T.D.A), review of final manuscript (T.D.A, M.R.G, P.S., J.E.S., B.A.I) and acquisition of funding (T.D.A, P.S., B.A.I).

## Funding

These studies were supported by grants from the National Institutes of Health P20GM135002 and U54GM104940, P30AG050911 to T.D.A. Support was also provided by the William Prescott (Pres) Foster Professorship and a grant from the Louisiana Board of Regents LEQSF(2024-25)-ENH-DE-03 to B.A.I. and the Louisiana State University Economic Development Assistantship to J.E.S. M.R.G. acknowledges the support from National Science Foundation (NSF CAREER award number: 2045640) and National Institute of General Medical Sciences (R35GM150564).

## Competing interests

The authors declare no competing interests.

## Additional information

**Supplementary Information** The online version contains supplementary material available at <https://doi.org/10.1038/s41598-024-75870-8>.

**Correspondence** and requests for materials should be addressed to T.D.A.

**Reprints and permissions information** is available at [www.nature.com/reprints](http://www.nature.com/reprints).

**Publisher's note** Springer Nature remains neutral with regard to jurisdictional claims in published maps and institutional affiliations.

**Open Access** This article is licensed under a Creative Commons Attribution-NonCommercial-NoDerivatives 4.0 International License, which permits any non-commercial use, sharing, distribution and reproduction in any medium or format, as long as you give appropriate credit to the original author(s) and the source, provide a link to the Creative Commons licence, and indicate if you modified the licensed material. You do not have permission under this licence to share adapted material derived from this article or parts of it. The images or other third party material in this article are included in the article's Creative Commons licence, unless indicated otherwise in a credit line to the material. If material is not included in the article's Creative Commons licence and your intended use is not permitted by statutory regulation or exceeds the permitted use, you will need to obtain permission directly from the copyright holder. To view a copy of this licence, visit <http://creativecommons.org/licenses/by-nc-nd/4.0/>.

© The Author(s) 2024